Electronic Supplementary Material (ESI) for Energy Advances.

The role of anionic processes in $Li_{1-x}Ni_{0.44}Mn_{1.56}O_4$ studied by resonant inelastic X-ray scattering

Felix Massel[1], Burak Aktekin[2], Yi-Sheng Liu[3], Jinghua Guo[3], Magnus Helgerud Sørby[4], Daniel Brandell[2], Reza Younesi[2], Maria Hahlin[1], and Laurent-Claudius Duda[1]

[1]*Department of Physics and Astronomy, Division of Molecular and Condensed Matter Physics, Uppsala University, Box 516, S-751 20 Uppsala, Sweden*

[2]*Department of Chemistry - Ångström Laboratory, Structural Chemistry, Uppsala University, Box 538, 751 21 Uppsala, Sweden*

[*]*Advanced Light Source, Lawrence Berkeley Laboratory, Berkeley, CA, USA*[3]*Advanced Light Source, Lawrence Berkeley Laboratory, Berkeley, CA, USA*[4]*Department for Neutron Materials Characterization, Institute for Energy Technology, P.Ø. Box 40, NO-2027 Kjeller, Norway*

November 14, 2022

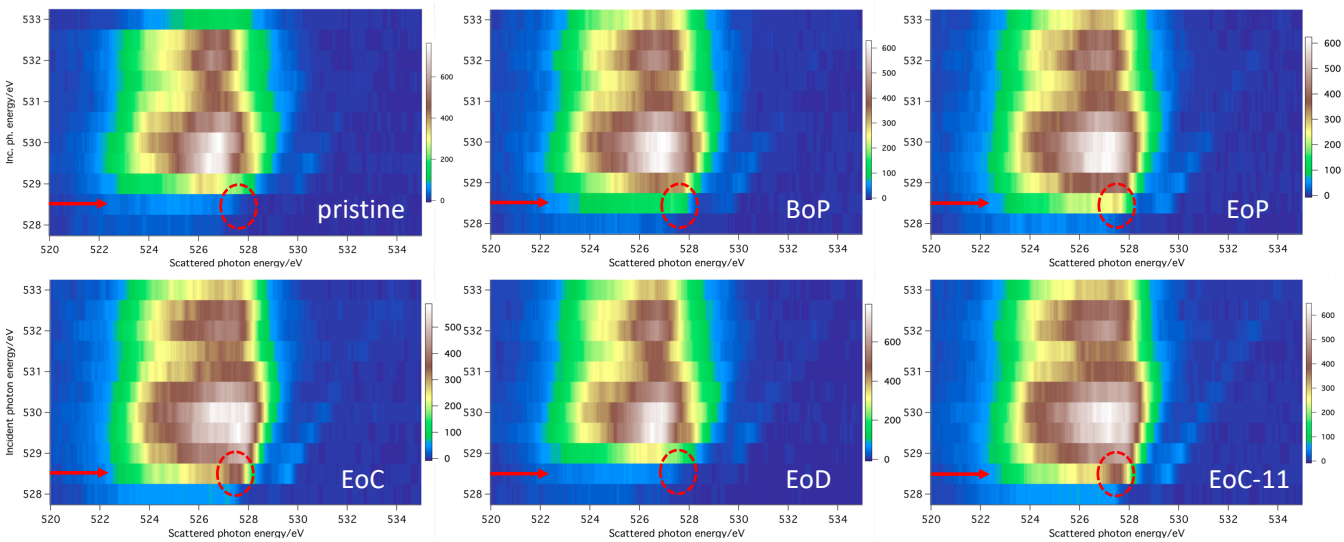

Fig. S1: Color-coded 2D O K RIXS maps for the first cycle (pristine, BoP, EoP, EoC, EoD) as well as an additional fully charged state in cycle 11 (EoC-11). The red arrows are level with the incident energy at which the Ni-O hybridization band RIXS signature (dashed red circles) appears.

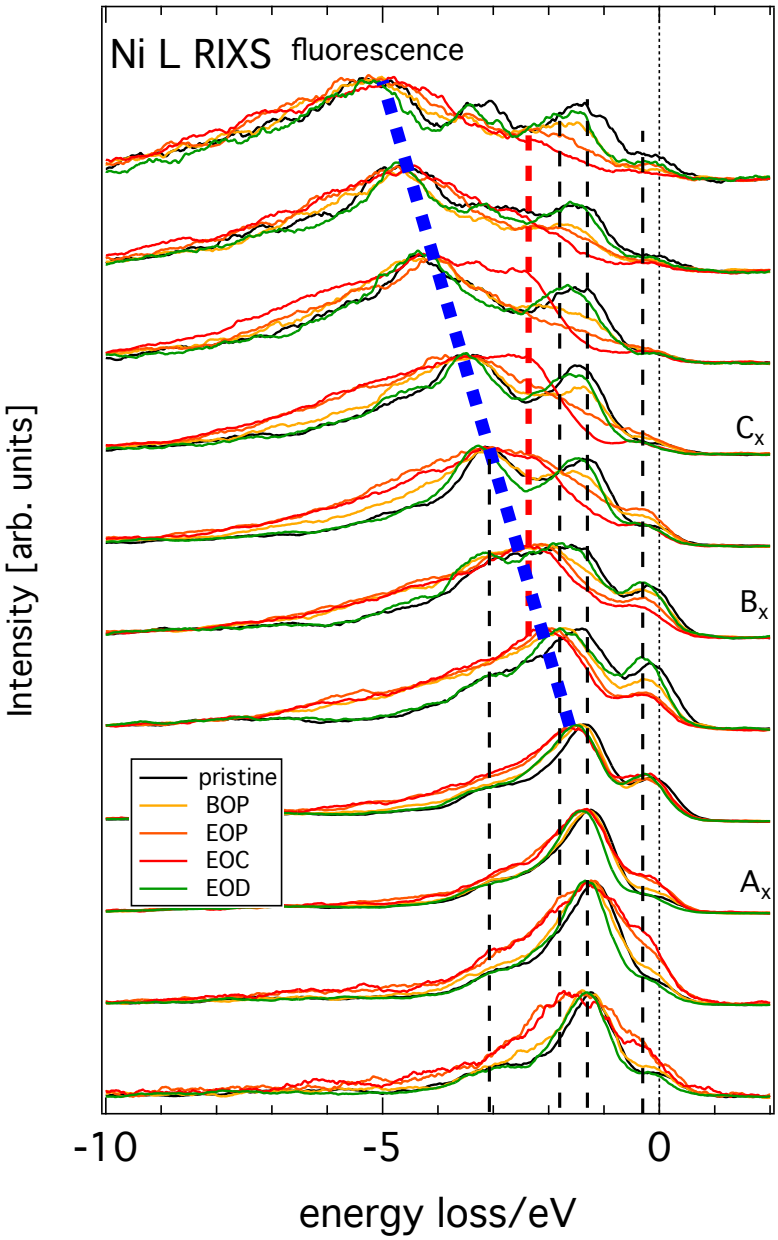

Fig. S2: Ni L-RIXS comparison waterfall plot of all states of charge for LMNO offset vertically for different incident energies (0.5 eV separation). The RIXS spectra excited with incident energies corresponding to the salient x-ray absorption features are indicated as A_x, B_x, C_x. The vertical dashed black lines indicate the salient energy loss features of a Ni $3d^8$ ground state whereas the vertical dashed red line is an emerging feature when LMNO becomes delithiated, belonging to a Ni $3d^{8-x}\underline{L}^{2-x}$ ground state. The slanted dashed blue line tracks fluorescence components (of non-constant energy loss) in the RIXS spectrum.

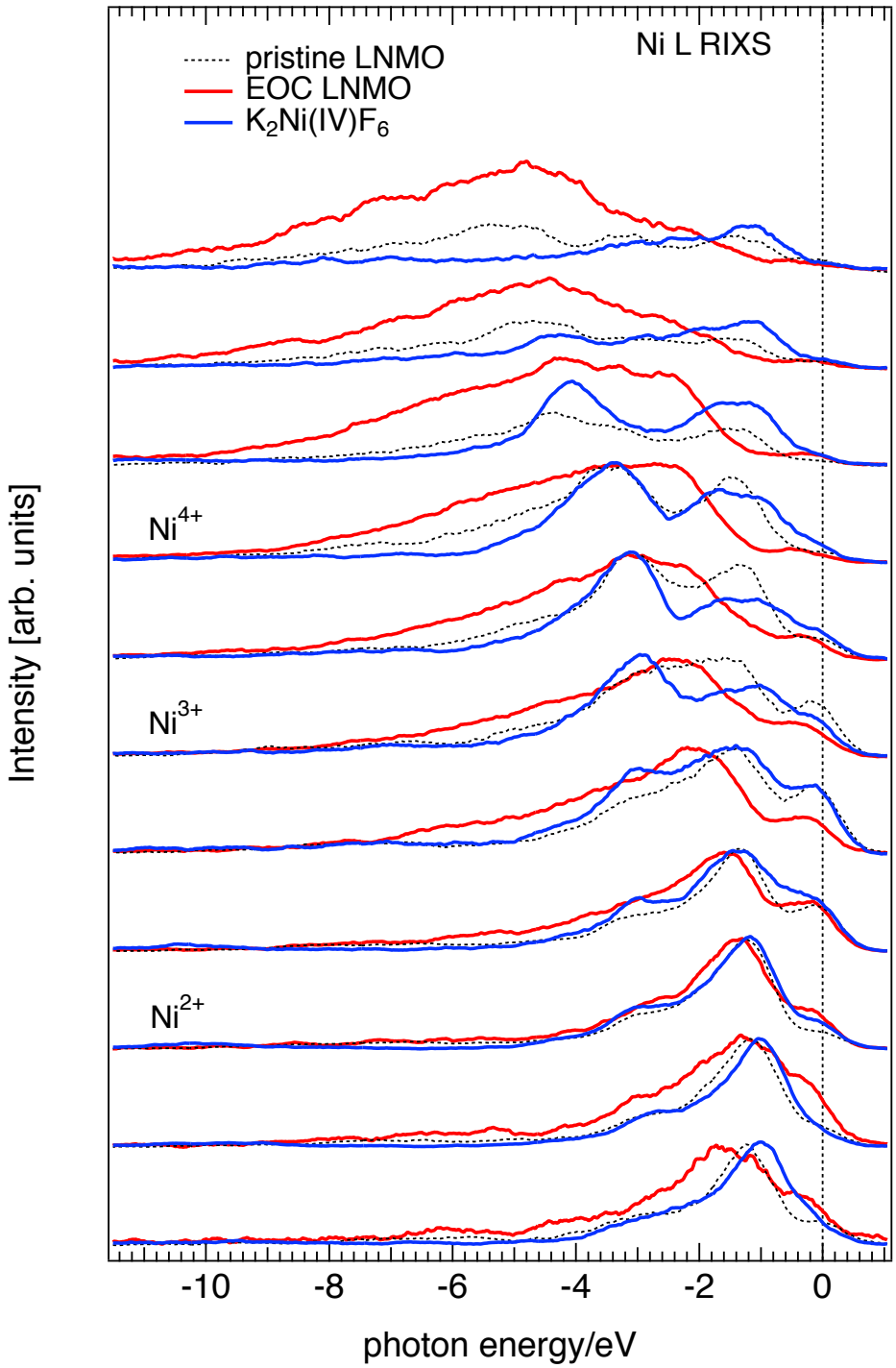

Fig. S3: Ni L-RIXS comparison waterfall plot of pristine LMNO, fully charged LMNO (EoC), and K_2NiF_6. K_2NiF_6 is an ionic reference compound for Ni^{4+}. K_2NiF_6 shows strong dd-excitations (<2 eV) expected for a $3d^6$-system (absent in EoC-LNMO).

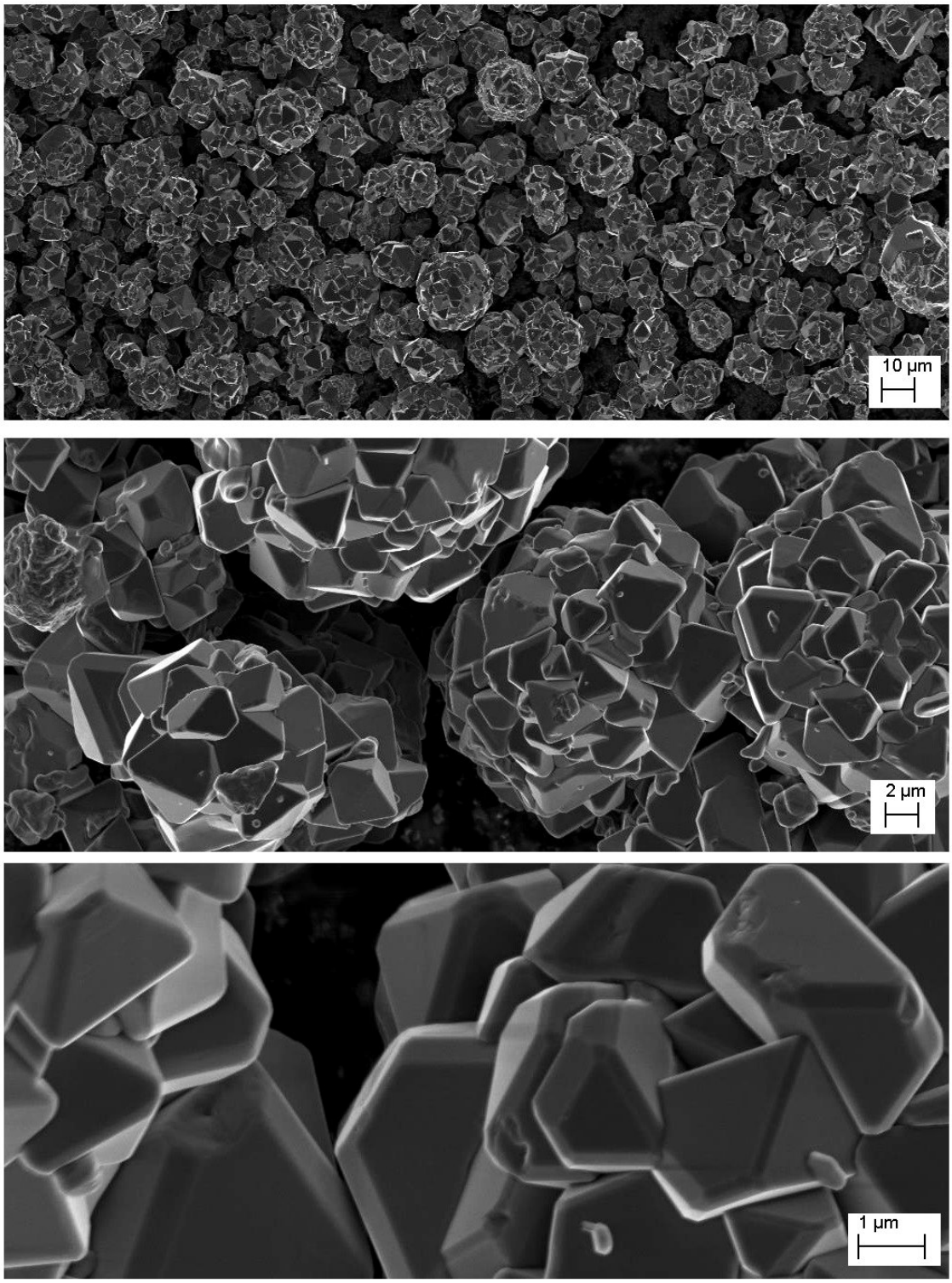

Fig. S4: SEM images of ordered LNMO powders used in this study are shown at various magnification scales.

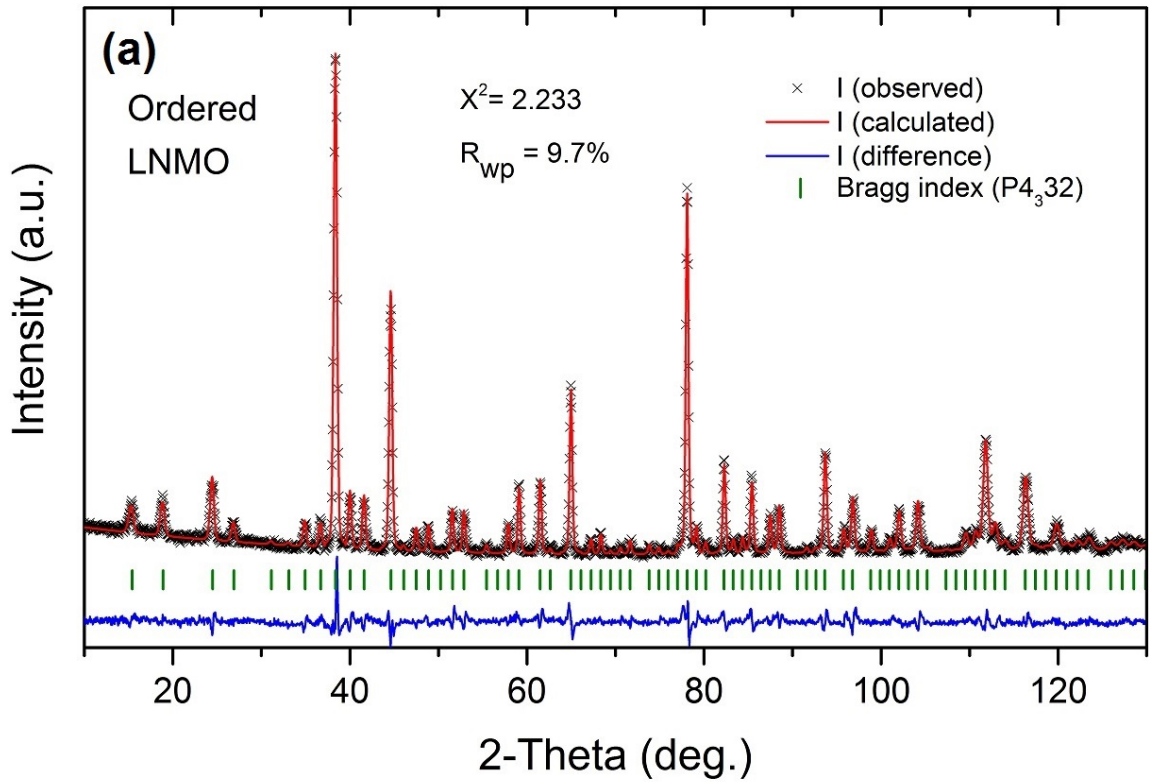

(b)

Wyckoff position	x	y	z	Occupancy	U_{iso} (Å^2)
Li – 8c	0.0039(12)	0.0039(12)	0.0039(12)	0.98(4)	0.013(4)
Mn – 4a	0.625	0.625	0.625	0.214(5)	0.010(1)
Ni – 4a	0.625	0.625	0.625	0.786(5)	0.010(1)
Mn – 12d	0.125	0.3813(7)	-0.1313(7)	0.969(2)	0.004(1)
Ni – 12d	0.125	0.3813(7)	-0.1313(7)	0.031(2)	0.004(1)
O – 8c	0.3860(3)	0.3860(3)	0.3860(3)	1	0.009(1)
O – 24e	0.1471(3)	-0.1412(3)	0.1268(3)	1	0.011(0)
P4₃32, a=b=c=8.1831(1), χ2 = 2.233, Rp = 7.5%, wRp = 9.7%.					

Fig. S5: (a) Neutron diffraction pattern of ordered LNMO powders used in this study are shown together with the calculated pattern from the Rietveld refinement. (b) Structural parameters obtained from the Rietveld refinement.

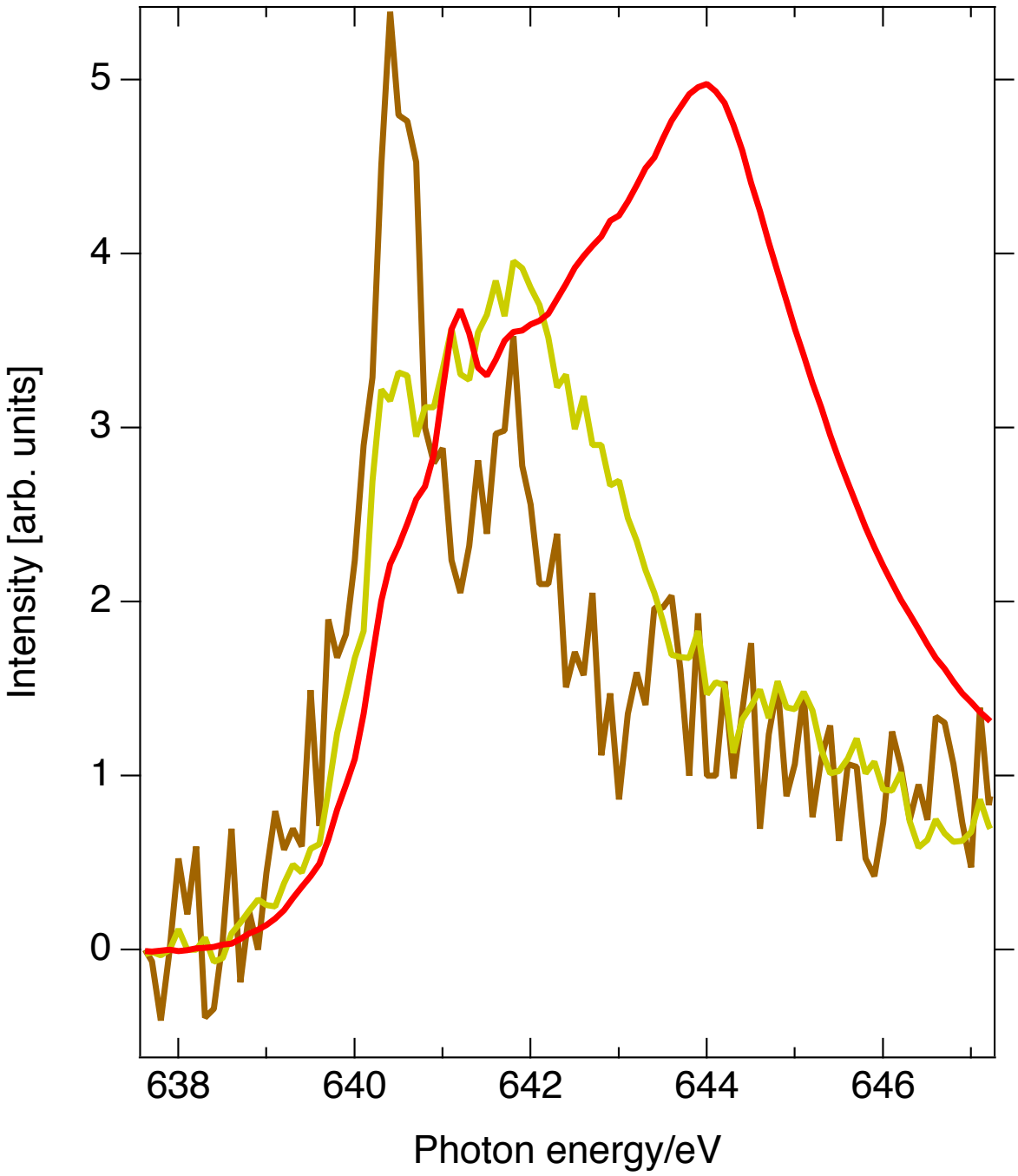

Fig. S6: Total electron yield spectra from the reference samples $Mn(NO)_3{\cdot}4H_2O$) (Mn^{2+}), Mn_2O_3 (Mn^{3+}), and MnO_4 (Mn^{4+}) recorded simultaneously as the IPFY spectra in Fig. 2a.